

Keywords or phrases:

Live-cell analysis, phenotypic screening, Artificial intelligence (AI), cell health, cytotoxicity, cell growth, cell cycle, mitochondrial membrane potential

Cell-based phenotypic screening with Incucyte® Live-Cell Analysis Systems

Gillian Lovell¹, Jasmine Trigg¹, John Rauch², Nicola Bevan¹

1. Sartorius UK, Royston, Hertfordshire

2. Sartorius NA, Ann Arbor, MI

Correspondence

Email: AskAScientist@sartorius.com

Introduction

Phenotypic screening – the measurement of a defined output in cells exposed to a large number of chemical compounds – is a vital tool in drug discovery, enabling scientists to rapidly identify potential drugs early in the discovery pipeline.¹ Live-cell imaging provides vastly more biological information than a single endpoint readout², since images reveal insight into growth and morphology changes of cells which are maintained within a physiologically relevant environment. Here we describe the application of Incucyte® Live-Cell Analysis Systems to derive insights into a library of 880 FDA-approved drugs by integrating data from label-free image analysis with quantification of fluorescent reporters.

Assay Principle

To perform the screening assay, A549 adenocarcinoma cells were seeded into 11 x 96-well microplates and once adhered, treated with a 1:1000 dilution of all compounds from the FDA-Approved Drugs Screening Library (Cayman Chemical #23538) supplied at 10 mM in DMSO (final concentration of all compounds 10 μ M). Microplates were placed into Incucyte® Live-Cell Analysis Systems where phase contrast and fluorescence images were acquired and analyzed using integrated software

To extract maximal information from each assay fluorescence readouts were multiplexed. In an Incucyte® SX5, A549 cells expressing the Incucyte® Cell Cycle Green/Orange reporter were combined with Incucyte® Annexin V NIR Dye; A549 cells expressing the nuclear marker Incucyte® Nuclight NIR Lentivirus were multiplexed with Incucyte® Caspase 3/7 Dye and Incucyte® Mitochondrial Membrane Potential (MMP) Dye. In an Incucyte® S3, A549 cells expressing the Incucyte® Kinase Akt Green/Red biosensor were used. In total, this screen was comprised of three runs wherein 11 x 96-well microplates of cells were treated with 80 test compounds per plate, and images were acquired every 2 hours for 4 days resulting in over 150,000 images.

Incucyte® Live-Cell Imaging

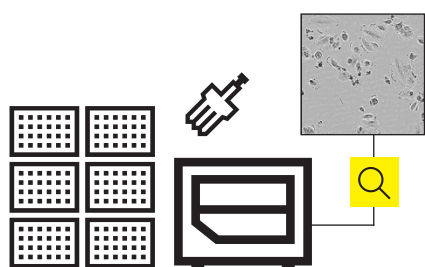
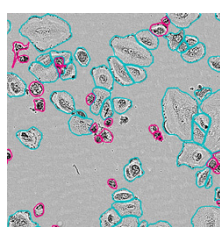
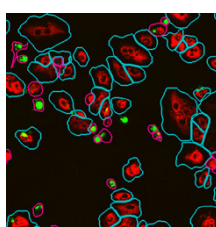


Image Analysis



Label-free



Fluorescence

Insight

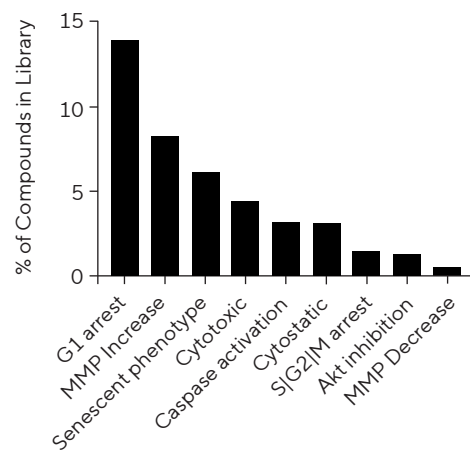


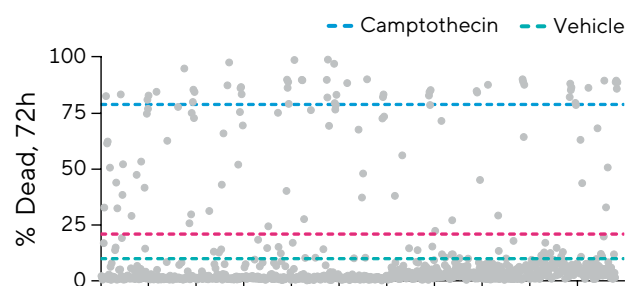
Figure 1: Phenotypic screening using Incucyte® Live-Cell Analysis Systems provides insight into compound mechanisms of action.

Data Analysis and Initial Hit Identification

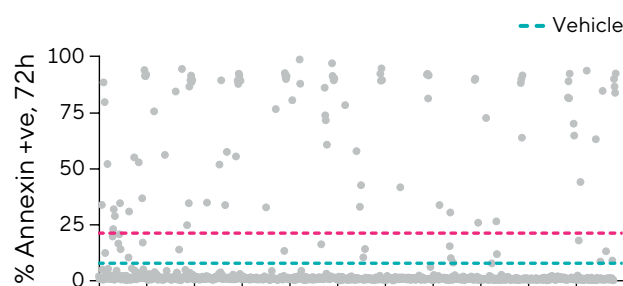
To achieve an overview of compound effects, an endpoint analysis was performed using each readout. Controls were included (vehicle, DMSO 0.1% and camptothecin, 10 μ M) to delineate the assay window and ensure assay robustness. Figure 2 displays scatter plots with each point representing a single concentration of each test compound with dashed lines indicating the mean values of the vehicle and appropriate controls. This visualization highlights the different ways in which drugs can affect cells – for example while a large number induce G1 arrest, many fewer are cytotoxic. Reporting multiple readouts can enable insight into the complexities of drug interactions with cells.

Appropriate time points were chosen based on the kinetic response of each readout. For example, time courses of % death showed maximal response between 48 and 72 hours while mitochondrial membrane and Akt kinase perturbation occurs within 12 hours. Cytotoxicity was quantified across all assay plates using Incucyte® AI Cell Health Analysis Software Module which segments cells and automatically performs label-free live|dead classification. Camptothecin was included as a positive control for cytotoxicity on every assay plate and induced an average of 79% cell death per image at 72 hours post treatment. Within the compound library, 39 out of 880 compounds induced greater than 50% cell death.

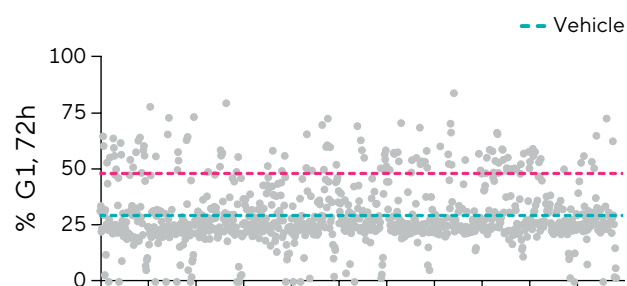
Cytotoxicity: AI Cell Health



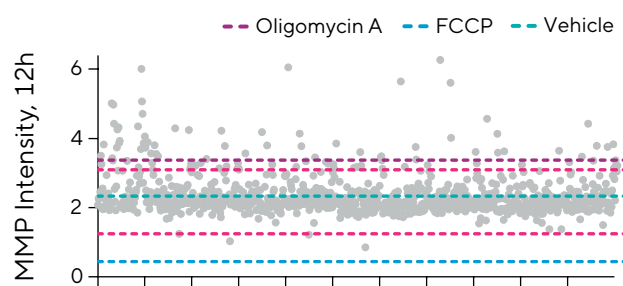
Apoptosis (Annexin V)



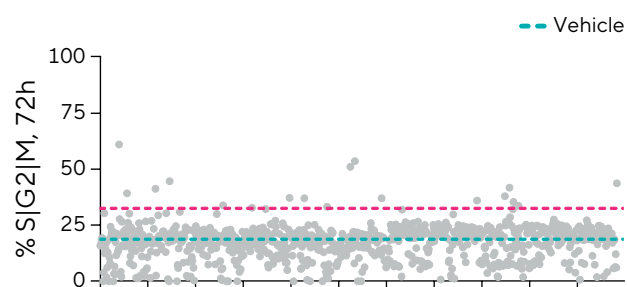
Cell Cycle Arrest (G1)



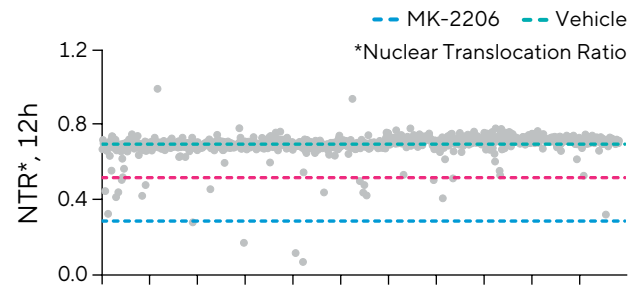
Mitochondrial Membrane Potential



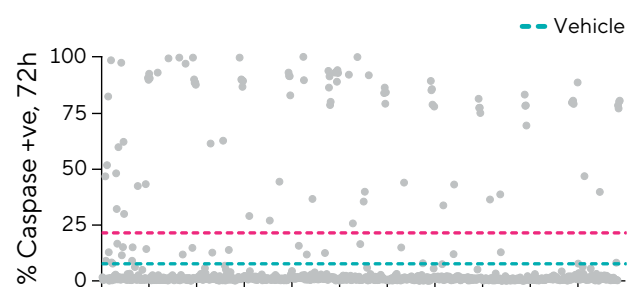
Cell Cycle Arrest (S|G2|M)



Akt Activity



Caspase Activating



Cell Enlargement >1800 μ m²

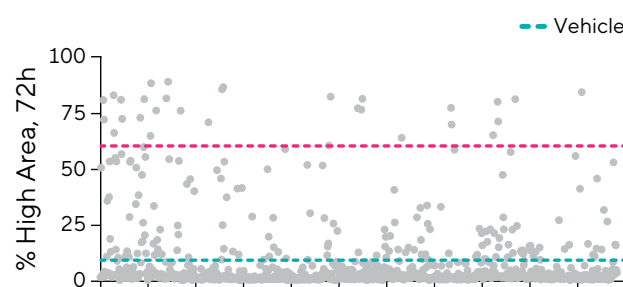


Figure 2: Scatter plots display endpoint analyses used to identify hits based on individual readouts at 72h. Teal line indicates the mean vehicle control values and magenta line denotes mean of vehicle ± 3 standard deviations. Control compounds are denoted in blue and purple.

Cells expressing the Incucyte® Cell Cycle reporter display green fluorescence in S|G2|M and orange fluorescence in G1 stage of the cell cycle. The percentage of cells in each stage were quantified by classifying the fluorescence within the live cell population only, since dead cells exit the cell cycle and can skew the data. Of the compounds within the library, 122 induced an increase in %G1 cells that exceeded the vehicle mean +3 standard deviations (~50% cells in G1) while only 13 induced a similar increase in %S|G2|M. Mitochondrial stress was evaluated using the Incucyte® Mitochondrial Membrane Potential (MMP) Assay. Changes in MMP alter the fluorescence intensity with control compound Oligomycin A inducing hyperpolarization (increase in Orange Mean Intensity within the cell boundary), while control compound FCCP induces depolarization (decrease in Orange Mean Intensity). 73 compounds from the library induced hyperpolarization while only 3 induced significant depolarization.

Activity of the kinase Akt was measured using cells expressing the Incucyte® Kinase Akt reporter. Basic fluorescence segmentation was used to identify the nucleus (red fluorescence, nuclear-restricted) and the localization of Akt substrate (green fluorescence) which translocates from the cytoplasm to the nucleus upon inhibition of Akt. The overlapping fluorescence masks are used to automatically quantify a Nuclear Translocation Ratio. In total 40 compounds from the library reduced the Nuclear Translocation Ratio below the vehicle mean -3 standard deviations.

Cell Growth and Cytotoxicity

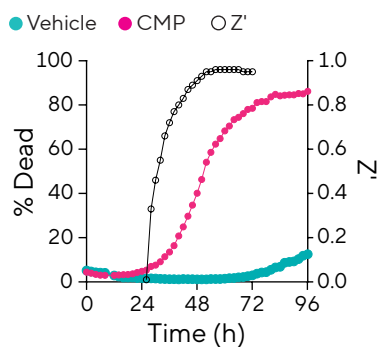
Positive control compound camptothecin induced cell death with the percentage of dead cells increasing from around 24 hours post treatment, reaching a plateau after 72 hours (Figure 3A). In negative control (vehicle) wells, a minimal level of death is observed until 72 hours when cells become overconfluent and begin to lose viability.

These controls were used to calculate Z' - a recognized measure of assay quality in which values >0.4 indicate robust results suitable for single-shot screening assays- and highlighted strong separation between positive and negative control values between 48 and 72 hours. Microplate views display percent dead cells vs time for every well and enable rapid, simple visualization of compound cytotoxicity. Figure 3B displays kinetic responses over 72 hours for all 80 test compounds on Plate 11 (gray, columns 2-11) and shows that 7 compounds on this plate induce cell death.

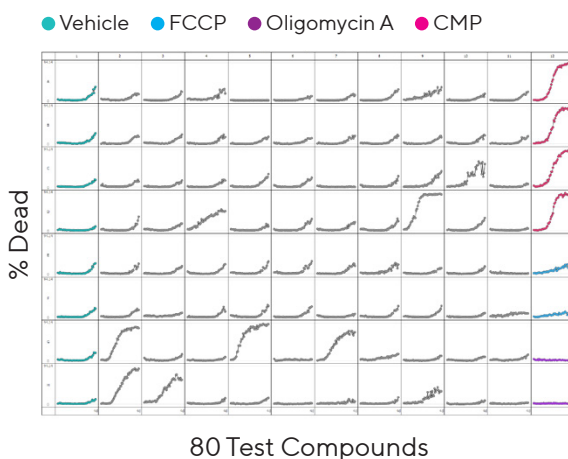
The compounds included in this screening assay possess a wide variety of mechanisms of action, and cellular response can be grouped into phenotypes by examining the correlation between cell growth and viability. Figure 3C displays the quantification of confluence (cell growth) and live cells (viability) at 3 days post-treatment with each point representing a single compound within the screen. Compounds which show results in the top right area of the plot (teal box) display high viability and high confluence, indicating that the cells grow normally and are unperturbed. Those compounds with results in the bottom left area of the plot (magenta box) display low viability and low confluence, indicating cytotoxic mechanisms of action. A cytostatic mechanism is indicated in compounds which sit in the top middle area since the viability of cells is high - meaning the compound has not induced cell death - while the confluence is distinctly lower than the non-perturbing compounds - meaning that the cell growth has been inhibited.

To examine the efficacy of the most potent cytotoxic compounds, a cell death assay was performed in a 384-well microplate using concentration ranges of camptothecin and the 11 compounds with highest % death at 72 hours. Figure 4A displays the label-free % Dead cells vs time for each concentration range (1 nM - 10 μ M; 1:3 serial dilution) and provides an overview of drug efficacy. While concentration dependence is observed for many of the compounds, both Panobinostat and Bortezomib induced a high level of cell death even at the lowest concentration of 1 nM.

A. % Dead Cells and Z' vs Time



B. % Dead Cells vs Time (All Cell Health)



C. Live Cells vs Confluence

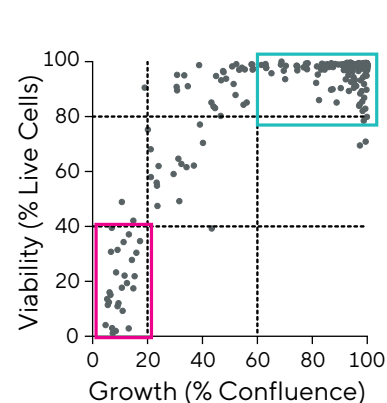
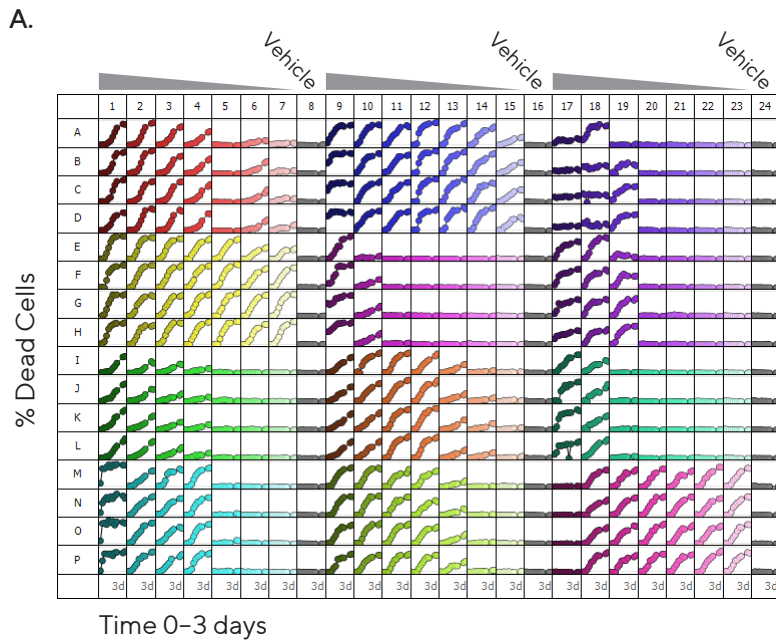


Figure 3: Data patterns indicate compound effect on cell growth and viability. Time course (A) displays % dead cells for vehicle and camptothecin; Z' value reaches a maximal value between 48 and 72h. Plate view (B) shows an overview of % dead cells over time for all wells of Plate 11. Scatter plot (C) shows correlation between cell growth and viability at 72h.



B.

Compound	Target	LogEC ₅₀
Camptothecin	Topoisomerase I	-7.1
Topotecan	Topoisomerase I	-5.7
Daunorubicin	Topoisomerase II	-6.8
Mitoxantrone	Topoisomerase II	-7.0
Idarubicin	Topoisomerase II	-7.9
Ceritinib	Kinase-ALK	-6.1
Vandetanib	Kinase-multiple	-5.3
LY2835219	Kinase-CDK 4/6	-6.0
Afatinib	Kinase-ErbB family	-5.7
MLN9708	20s Proteasome	-6.8
Bortezomib	20s Proteasome	N/C
Panobinostat	Histone deacetylase	N/C

C.

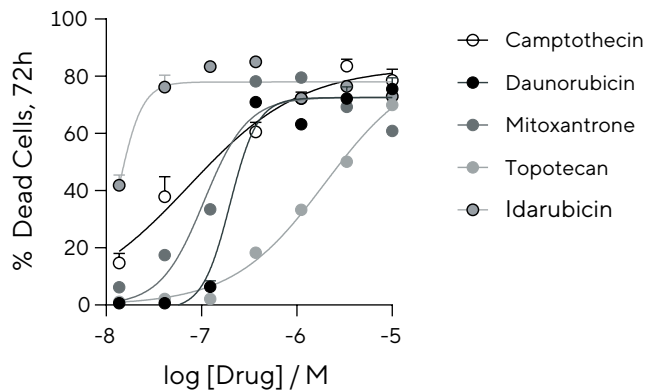


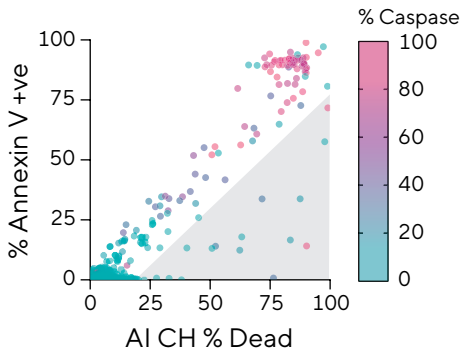
Figure 4: Efficacy of the 11 most toxic compounds is determined using Incucyte® AI Cell Health Analysis. Plate view displays % Dead cells versus time (A), and calculated compound efficacy was calculated (B). Concentration response curves are shown for topoisomerase I and II inhibitors (C).

Log EC₅₀ values for each tested compound are shown in Table 4B along with the mechanisms of action which included topoisomerase inhibitors, kinase inhibitors, and 20s Proteasome inhibitors. Figure 4C overlays the concentration response curves of the topoisomerase I and II inhibitors which reveals that the most potent is Idarubicin, and the least potent is Topotecan.

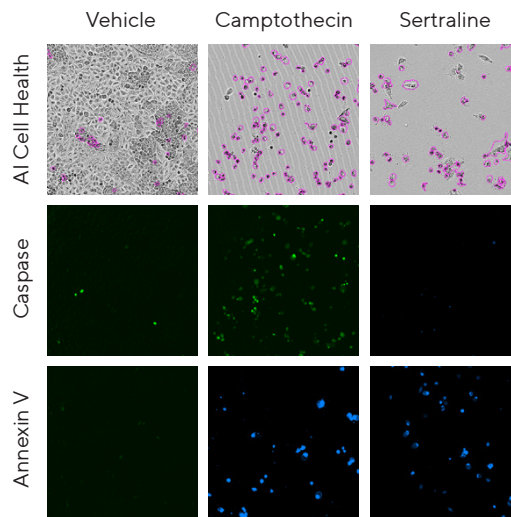
Cell death can occur via several mechanisms including necrosis and apoptosis – and within these are sub-types such as caspase-dependent versus caspase-independent apoptosis.³ To elicit more information on these mechanisms of cell death we included Incucyte® Annexin V Dye (high fluorescence indicates apoptosis) and Incucyte® Caspase 3/7 Dye (high fluorescence indicates caspase-dependent apoptosis). Figure 5A displays the correlation between total cell death (x axis, AI CH % Dead), apoptosis (y axis, % Annexin V positive) and caspase dependence (colour scale from teal to magenta, % Caspase positive). The scatter plot shows

a high correlation between total cell death and Annexin V ($R^2 = 0.95$) with only 2 % of compounds diverging from this relationship (17 out of 880 compounds). Although many apoptotic compounds are caspase-positive, Sertraline appears to act via caspase-independent pathways. Images (5B) and bar graph (5C) show quantification of using Incucyte® AI Cell Health (top row), Incucyte®Caspase 3/7 Dye (middle row) and Incucyte®Annexin V Dye (bottom row) response at 3 days post treatment. Untreated cells show high confluence with a small number of dead cells within the image, and low fluorescence response from both Incucyte® Caspase 3/7 and Annexin V Dyes. Camptothecin, a topoisomerase II inhibitor, shows a high level of cell death across all readouts indicating caspase-dependent apoptosis. Sertraline induces apoptotic cell death as indicated by AI Cell Health analysis and Incucyte® Annexin V response. However, within the dead cells the Incucyte® Caspase 3/7 intensity was low, indicating a caspase-independent apoptotic pathway.

A. Cell Death Mechanisms



B. Fluorescent Apoptosis Reagents



C. Quantification of Reagent Response

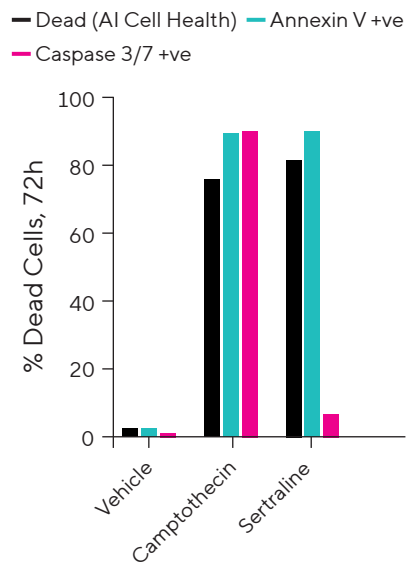


Figure 5: Cell death mechanisms can be elucidated by combining label-free analysis with fluorescence reagents. Annexin V positive and Caspase 3/7 positive cells were identified by performing fluorescence classification. Scatter plot (A) correlates (AI Cell Health % Dead) and apoptosis (% Annexin V positive) and colour scale highlights caspase activating compounds (% Caspase 3/7 positive). Images (B) display AI Cell Health dead cell classification (magenta outline, top row), caspase 3/7 activity (green fluorescence, middle) and Annexin V binding (Near IR fluorescence, bottom row). Bar graph (C) indicates quantification of these responses at 72h.

Cell Cycle Arrest

To explore the effect of compounds on cell cycle progression cells expressing the Incucyte® Cell Cycle Lentivirus were used. For quantification, an initial AI Cell Health analysis was performed and subsequently the live cell population was classified according to green and orange fluorescence intensity to identify cells in S|G2|M and G1 respectively. By excluding dead cells from this analysis the data is focused solely on live cells which are still within the cycle.

The endpoint analysis in Figure 2 shows that while numerous compounds arrest the cycle in G1, very few arrest in S|G2|M. Further examination of the kinetic response provides additional insight into individual compound effects. Figure 6 shows the cells in G1 (orange) and S|G2|M (green) for untreated (vehicle) cells, as well as cells in the presence of Mycophenolic acid or Flumazenil.

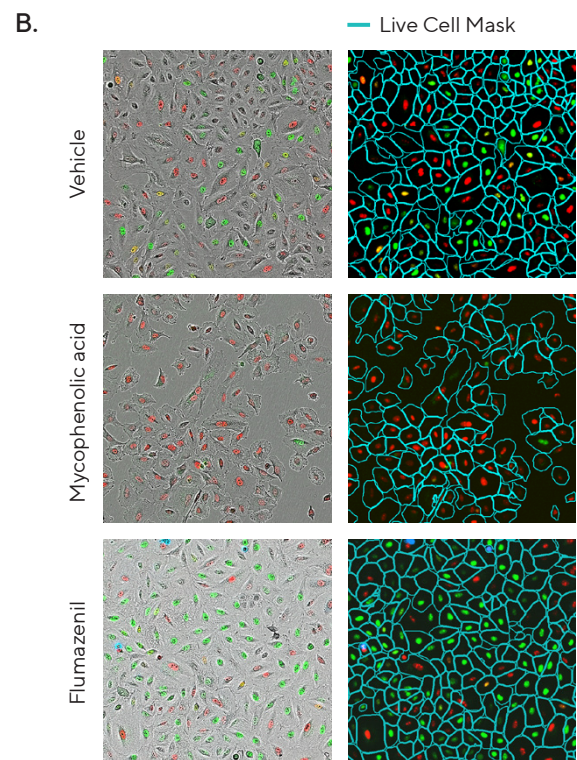
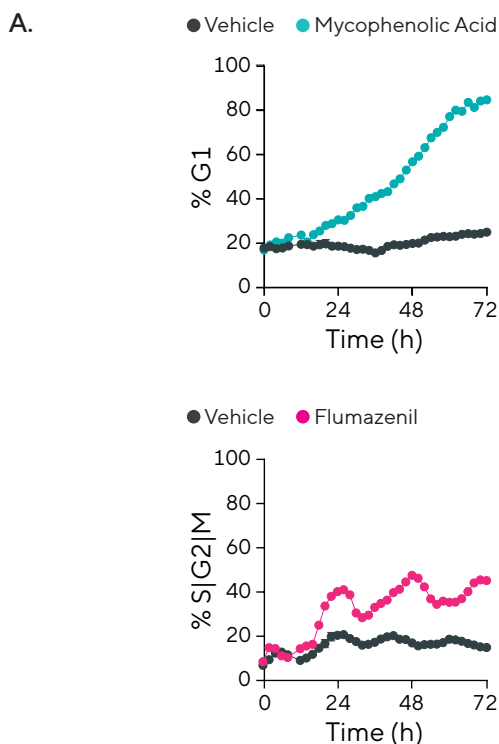


Figure 6: Cell cycle arrest is induced by a subset of compounds. Time courses (A) show the effect of Mycophenolic acid on %G1 (top) and that of Flumazenil on %S|G2|M (bottom). Images (B) show healthy cell morphology in phase contrast and fluorescence within the live cell population (teal segmentation).

Mycophenolic acid inhibits nucleotide synthesis (occurring in S phase), causing the cells to accumulate in G1. Figure 6A shows that in the presence of mycophenolic acid, the % G1 cells (orange) increases between 24 and 72 hours. Flumazenil is an antagonist of GABA_A receptors which lie upstream of several signaling pathways relating to cell growth. Figure 6A demonstrates that in the presence of Flumazenil an increase in the % S|G2|M cells is observed. Unlike Mycophenolic acid which induces a sustained increase over time in % G1, the presence of flumazenil induces an elevated % S|G2|M population which oscillates over time. This oscillation is observed when cells are treated with compounds which elongate mitosis and cause the cells to divide almost synchronously, creating peaks and troughs in the cell cycle populations.

Mitochondrial Membrane Potential

Mitochondrial stress is an early indicator of cell perturbation⁴, therefore the Incucyte® MMP Orange Dye was used to measure the effect of the compounds on mitochondrial membrane potential. The time course in Figure 7A quantifies MMP intensity within all segmented cells over time and shows that control compounds FCCP and Oligomycin A induce membrane depolarization and hyperpolarization, respectively. Cefdinir – a cephalosporin-based antibiotic – is shown to induce rapid hyperpolarization to a greater extent than Oligomycin A. Busulfan – a DNA alkylating agent – causes membrane depolarization almost as strongly as FCCP however the kinetic plot indicates that the depolarization process occurs more slowly.

Images (Figure 7B) show the fluorescence within the cell boundaries at 12 hours post-treatment with teal mask indicating live cells and magenta indicating dead cells. Depolarization results in loss of fluorescence intensity while hyperpolarization yields an increase in fluorescence intensity relative to vehicle, with little change in cell morphology in both cases. At this early timepoint (12h) minimal cell death is observed, and the scatter plot (Figure 7C) reveals little correlation between mitochondrial membrane polarization at 12 hours and eventual cell death at 72 hours.

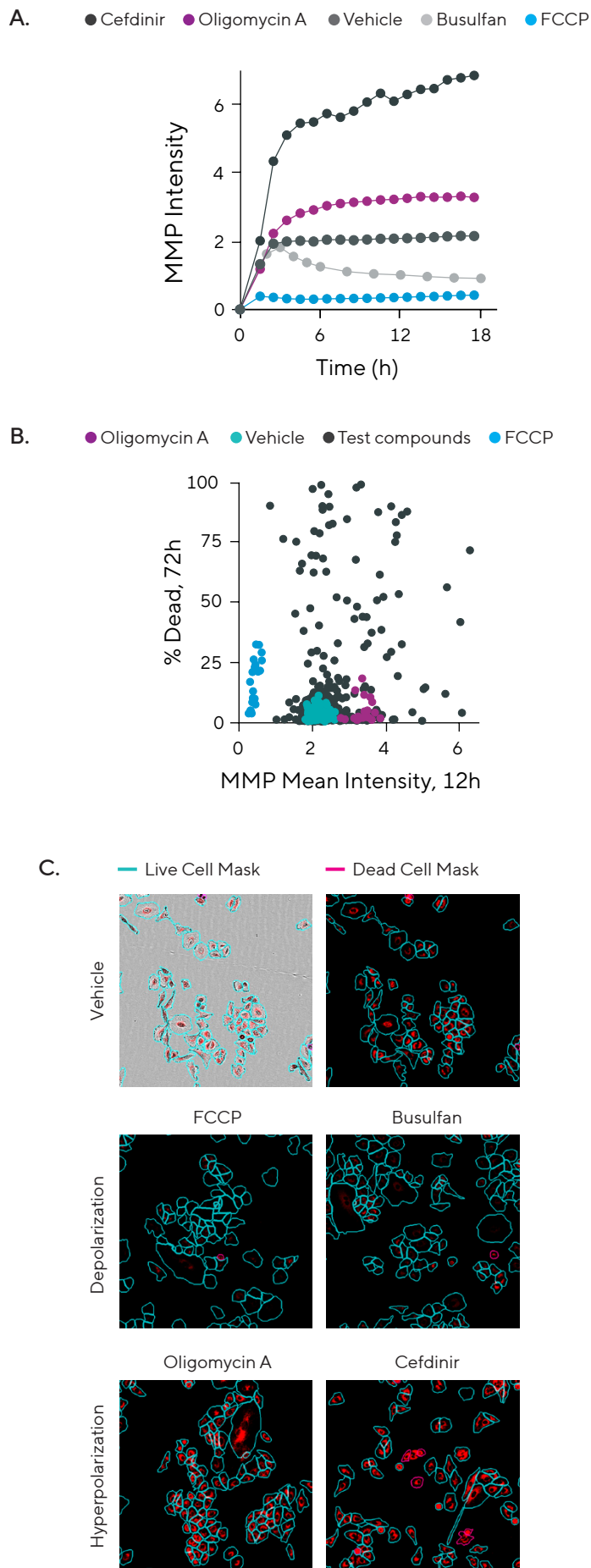


Figure 7: Perturbance of cellular mitochondrial membrane potential (MMP). Time course of MMP intensity (A) highlights depolarization (loss of intensity relative to vehicle) and hyperpolarization (increased intensity relative to vehicle). Images (B) show fluorescence within the cell boundaries at 12h. Scatter plot (C) correlates MMP at 12h with cell death at 72h.

Akt Kinase Inhibition

Kinase signaling is a critical regulator of cell proliferation, metabolism, and apoptosis.⁵ To identify potential kinase inhibitors within the compound library, cells expressing the Incucyte® Kinase Akt biosensor were used and kinase activity was quantified by measuring the nuclear localization of the fluorescent Akt substrate (Nuclear Translocation Ratio, NTR).

Cells with inhibited Akt activity display a reduced NTR value and the initial hit scatter plot in Figure 2 shows that 20 out of 880 total compounds decrease the NTR beyond 3 standard deviations below the mean vehicle value. However, cell morphology analysis reveals that some of these compounds induce cell rounding, meaning that the localization of the fluorescent Akt substrate between the nucleus and cytoplasm cannot be robustly determined. Cell rounding forces all the green fluorescence to overlap with the nucleus (red fluorescence). To identify Akt inhibitors more accurately the NTR value was plotted against cell eccentricity – a measure of cell elongation which decreases as cells become rounded.

Figure 8A shows a correlation between eccentricity and NTR (black diagonal line) of cells treated with vehicle or test compounds; a separate control assay was performed using specific Akt inhibitor MK2206 and the result is included in blue. Compounds which induce a decreased NTR without rounding (gray shaded area) are “true” hits since the fluorescence localization can be accurately measured.

Figure 8B displays an example of true Akt inhibition (AZD 9291) and cell rounding (Auranofin). AZD 9291 treatment causes the green fluorescent Akt substrate to localize within the nucleus (indicated by the red outline) and the NTR is reduced, however the cells have a similar eccentricity value to vehicle. Auranofin treated cells experience a reduction in NTR however since the eccentricity also drops and cells visibly round up, this compound is discarded as a hit.

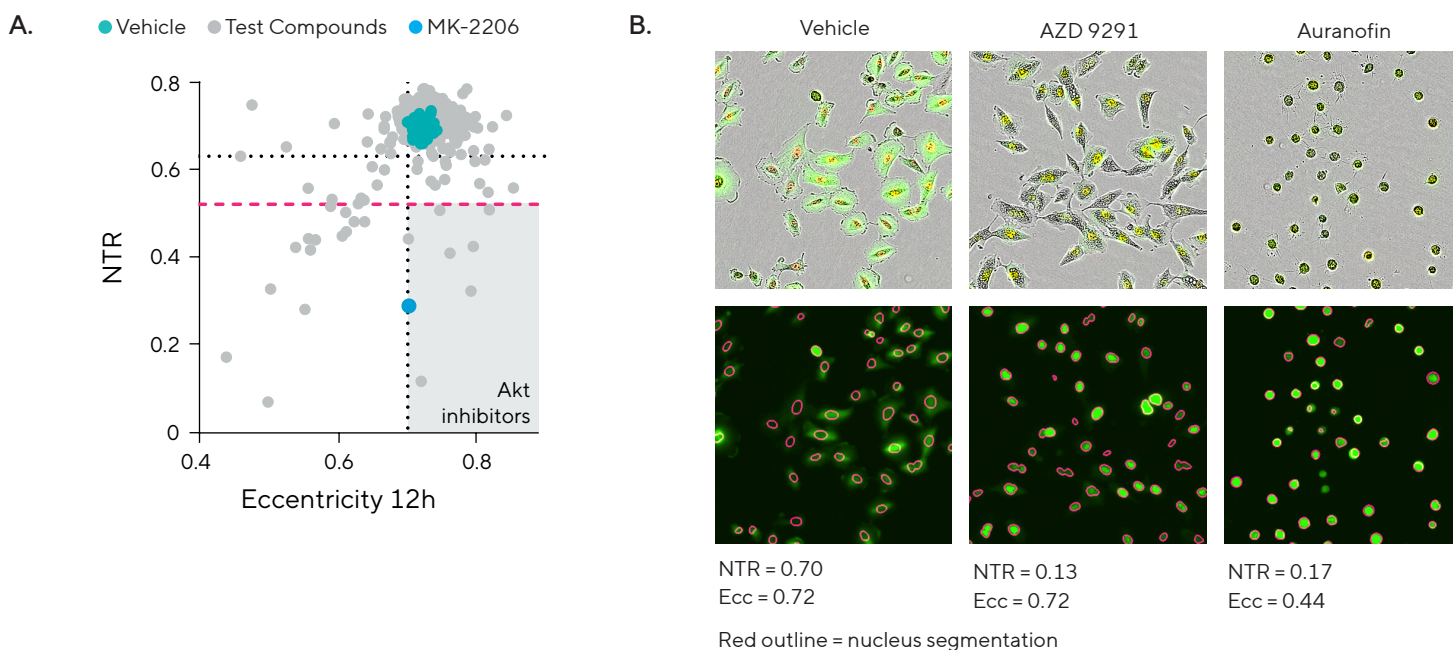


Figure 8: Inhibition of Akt kinase activity. Scatter plot (A) relating Nuclear Translocation Ratio (NTR) to eccentricity (Ecc) indicates positive hits for Akt inhibitors. Images (B) compare true inhibition by AZD 9291 to false positive Auranofin.

Summary and Conclusion

Incucyte® Live-Cell Analysis Systems were used to perform phenotypic screening of an 880-compound library. An overview of compound activity was obtained using endpoint analysis of images capturing multiple readouts including label-free cell death analysis, fluorescent apoptosis and mitochondrial membrane potential reagents, and fluorescent reporters measuring cell cycle stage and Akt kinase activity.

Kinetic information gained by repeated image acquisition within a physiologically relevant environment added insight into the dynamic changes which are often overlooked using end-point analysis alone. Additionally, by combining multiple readouts compound mechanisms were elucidated and misleading results were discarded. These data are reinforced with cell images throughout the time course that demonstrate any morphological changes yielding highly robust and insightful data.

References

1. Opportunities and challenges in phenotypic drug discovery: an industry perspective. Moffat, John G, et al. 2017, *Nature Reviews Drug Discovery*, Vol. 16, pp. 531 - 543.
2. Live-cell imaging: The cell's perspective. Cole, Richard. 5, 2014, *Cell Adhesion and Migration*, Vol. 8, pp. 452 - 459.
3. Cell Death in the Origin and Treatment of Cancer. Strasser, Andreas and Vaux, David L. 2020, *Molecular Cell*, Vol. 78, pp. 1045 - 1054.
4. Systemic effects of mitochondrial stress. Bar-Ziv, Raz, Bolas, Theodore and Dillin, Andrew. 6, 2020, *EMBO Reports*, Vol. 21, p. e50094.
5. AKT as a Therapeutic Target for Cancer. Song, Mengqui, et al. 6, 2019, *Cancer Research*, Vol. 79, pp. 1019 - 1031.

North America

Sartorius Corporation
300 West Morgan Road
Ann Arbor, Michigan 48108
USA
Phone +1 734 769 1600
Email: orders.US07@sartorius.com

Europe

Sartorius UK Ltd.
Longmead Business Centre
Blenheim Road
Epsom
Surrey, KT19 9QQ
United Kingdom
Phone +44 1763 227400
Email: euorders.UK03@sartorius.com

Asia Pacific

Sartorius Japan K.K.
4th Floor, Daiwa Shinagawa North Bldg.
1-8-11, Kita-Shinagawa 1-chome
Shinagawa-Ku
Tokyo 140-0001
Japan
Phone +81 3 6478 5202
Email: orders.US07@sartorius.com

 **For further information, visit**
www.sartorius.com